Eur Biophys J (1986) 14:113–122

European Biophysics Journal


# Flow orientation of brain microtubules studied by linear dichroism

**J. Nordh[1]*, J. Deinum[2], and B. Nordén[1]**

[1] Department of Physical Chemistry, Chalmers University of Technology, S-41296 Göteborg, and
[2] Department of Medical Physics, University of Göteborg, S-400 33 Göteborg, Sweden

Received December 28, 1984/Accepted in revised form April 14, 1986

**Abstract.** Flow orientation of bovine brain microtubules has been studied using phase-modulation detected linear dichroism, LD, in a Couette cell with radial light propagation. LD could be sensitively measured in a wide flow gradient interval: $10^{-3}$ – $10^{3}\,s^{-1}$, without any apparent degradation of the microtubule structure. An extremely small flow gradient, $10^{-3}\,s^{-1}$ is sufficient to give significant orientation, and $10\,s^{-1}$ rapidly produced a very high degree of orientation. It is also shown that thermal convection effectively orients microtubules in vitro.

The apparent linear dichroism is dominated by an anisotropic scattering from the aligned microtubules, superimposed on a weaker absorption dichroism due to intrinsic chromophores. The linear dichroism due to anisotropic turbidity, $LD^{\tau}$, is found to be an excellent tool for monitoring the formation of microtubules and in contrast to ordinary turbidity measurements, non-specific aggregates contribute to a far less extent.

Time resolved $LD^{\tau}$ was used to study the orientational relaxation of microtubules upon stopped shear. The relaxation towards random orientation can be described by a slow, multi-exponential decay. With increasing protein concentration the relaxation becomes slower and above approximately 1 mg/ml a fraction with a semipermanent orientation is formed. Finally, the development of orientation with time upon applying a small, constant gradient has been measured and the results are considered in terms of a model for flow orientation of rigid rods.

**Key words:** Microtubules, microtubule-interaction, assembly, orientation, linear dichroism, anisotropic turbidity

* To whom offprint requests should be sent

## Introduction

Microtubules (for a review see Dustin 1984) are hollow, cylindrical organelles, several μm long and approximately 25 nm in diameter, made up of 13 protofilaments of alpha-beta heterodimers of tubulin. On the microtubule wall microtubule-associated proteins, MAPs, are present. Microtubules are found in all eukaryotic cells where they are implicated in a variety of structural and dynamic roles: in cell shape, division, constituting the mitotic spindle, motility, transport and secretion. Many types of movements require the integrity of the microtubules and become impossible if the microtubules are disassembled, for example, by low temperature or through the action of drugs. An example is the rapid movement of proteins and secretory granules along the axons and the redistribution of mitochondria. Microtubules seen in the cell, by dark field microscopy or studied by electron microscopy often show a highly organized structure. For example, in the nerve cell the microtubules are found arranged parallel to the axon and also in the mitotic spindle the microtubules are specifically oriented. The cellular role of microtubules in the different cell processes is also likely to depend on their structural organisation.

Also in vitro, when assembled in solution, as seen on electron microscopy grids or in pelleted centrifuged material, microtubules are seldom completely randomly oriented (Dustin 1984). A relevant question is therefore what forces are needed to produce orientation? Another important question is the role of interactions between microtubules in solution. However, few techniques allow microtubule organization in solution to be studied under controlled conditions. In the majority of methods used to study microtubule assembly in vitro, perturbation of the solution structure generally implies spurious orientation effects.

In this report bovine brain microtubules in vitro have been studied by flow linear dichroism, a technique which can provide hydrodynamic as well as spectroscopic information on the structure of macromolecules in solution (Wilson and Schellman 1978; Nordén 1978). As will be shown very low shear forces are sufficient to induce highly ordered microtubule structures. Furthermore, stopped shear relaxation studies have given unique time resolved information on the microtubule-microtubule interaction and organization which cannot be obtained with convential techniques.

## Experimental

### *Microtubule preparation*

Microtubule proteins were prepared from bovine brain cortex in the absence of glycerol by three cycles of assembly-disassembly (Deinum et al. 1981; Borisy et al. 1974). The assembly buffer contained, 0.1 *M* Pipes, 1 m*M* GTP, 0.5 m*M* $MgSO_4$, 1 m*M* EGTA at pH 6.8. After the last disassembly step the microtubule solution was usually centrifuged at 200,000 *g* for 30 min at 4 °C and drop-frozen in liquid nitrogen.

Microtubule proteins devoid of the high molecular weight associated proteins were prepared by short time treatment of assembled microtubules with Sepharose-bound chymotrypsin (to be published).

### *Assembly*

Assembly of 0.05–2 mg/ml freshly thawed microtubule proteins in assembly buffer was started by increasing the temperature from 10° to 35 °C and the increase in turbidity (Gaskin et al. 1974) was monitored by the apparent increase in absorbance at 350 nm, $\Delta A^{\tau}$, relative to the absorbance at 4 °C and concomitantly by the appearance of a linear dichroism signal, $LD^{\tau}$ at 350 nm, upon orientation. Samples for electron microscopy were treated as described before (Deinum et al. 1985).

### *Protein concentration*

Microtubule protein concentration was determined with Bio-Rad's protein assay using Coomassie Brilliant Blue based on the method of Bradford (1976) as described before (Deinum et al. 1981).

### *Chemicals*

All chemicals were of reagent grade and only deionized distilled water was used.

### *Instrumentation*

Absorbance spectra were recorded on a Varian Cary 219 spectrophotometer and a Pye Unicam spectrophotometer was used for monitoring the turbidity at 350 nm. The temperature in the cell was maintained with a thermostated cell-holder.

Linear dichroism, defined as the absorption difference of linearly polarized light, $LD = A_{\parallel} - A_{\perp}$ (where $A_{\parallel}$ denotes the absorbance with the electric vector of light polarized parallel to the shear and $A_{\perp}$ the corresponding perpendicular absorbance), was measured differentially on a Jasco-J500 spectropolarimeter equipped with an achromatic quarter-wave device, allowing direct and time-resolved measurement of LD (Davidson and Nordén 1976; Nordén and Seth 1985). The modulation frequency of the instrument was 50 kHz. The dichrometer was connected on line to a Tektronix 4052 computer for data evaluation. Two types of thermostated Couette cells were used, one with an inner (Wada and Kozawa 1964) and one with an outer rotating cylinder (Fig. 1), both having a radial light-path of $2 \times 0.50$ mm. The cell with the inner-cylinder rotating was surrounded by a thermostated water jacket, while the cell with the outer-cylinder rotating had instead the static inner-cylinder thermostated. In the latter cell a thermal gradient could be produced at rest, e.g. with the inner-cylinder at 35 °C and the outer at ambient temperature of the cell compartment, generally 30 °C. The rotation-force, creating

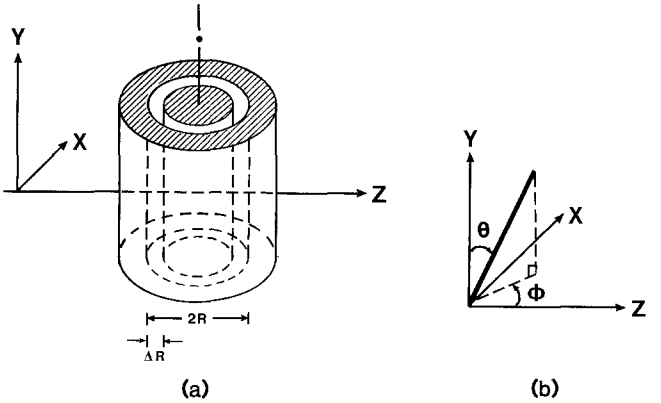


**Fig. 1 a and b.** Couette cell. **a** Cell geometry: $2R = 3$ cm, $\Delta R = 0.050 \pm 0.002$ cm, $Z$ = direction of propagation of light, $X$ = polarization direction $\parallel$ to the shear, $Y$ = polarization direction $\perp$ to the shear. **b** Orientation of a particle in the laboratory-fixed coordinate system

the gradient, was obtained with a home-made drive unit, employing an electronic feedback velocity control and an electro-mechanical brake.

The mechanical brake and the stopped-shear characteristics were tested on a solution of synthetic DNA, poly($dG-dC$) of 500 base pairs in which perfect random orientation was reached within 0.1 s. As the reorientation time for this polynucleotide is in the μs range (Fredericq and Houssier 1973), as also confirmed by us with electric dichroism, this shows that the time constant for the equipment was less than 0.1 s.

*Curve fitting*

The relaxation curves were fitted by 'derivative free non linear regression' (BMDPAR, University of California) to a multi-exponential function.

## Theory of linear dichroism

*Dichroic absorption*

The method of linear dichroism for the study of spectroscopic properties and structure of orientable, light-absorbing molecules is today well established (reviews: Hofrichter and Eaton 1976; Nordén 1978; Thulstrup 1980). Flow-orientation has been extensively used, for example, in the study of nucleic acids (Wilson and Schellman 1978; Nordén and Tjerneld 1982; Matsuoka and Nordén 1982). Linear dichroism, which originates from light absorption by an electronic or vibrational transition, for uniaxial orientation can be separated into an optical and an orientational factor:

$$\mathrm{LD}_r^A = S\,3/2\,(3\cos^2\alpha - 1) \quad (1)$$

$$\mathrm{LD}_r^A = \mathrm{LD}/A_{\mathrm{iso}}\,, \quad (2)$$

where the *reduced dichroism*, $\mathrm{LD}_r^A$ is defined as the linear dichroism divided by the absorbance of the isotropic sample. $S$ is an orientation function usually monotonically dependent on the strength of the orienting force-field. $S$ also depends on the symmetry of the orientational distribution and on the hydrodynamics and flexibility of the oriented molecules, etc. $S=0$ corresponds to complete random orientation and $S=1$ to perfect orientation. The geometry of the present shear field does not provide the required uniaxial symmetry, however, Eq. (1) is still valid as it can be assumed that each microtubule has, on the average, cylindrical rotation symmetry. The second factor of Eq. (1) is an optical factor with $\alpha$ being the angle between the light absorbing transition moment in the molecule and a local orientation axis, the microtubule cylinder axis. Eq. (1) applies only to $\mathrm{LD}_r^A$ from *light absorbing chromophores*, for example guanine of associated GTP in tubulin or other microtubule-associated chromophores. The main contribution to the linear dichroism of samples of aligned microtubules derives from polarized *light scattering* and will be denoted 'turbidity dichroism', $\mathrm{LD}^\tau$, to avoid confusion. (The term 'conservative dichroism', Meeten (1981), also occurs.) In contrast to ordinary absorbance, the measurement of absorption dichroism, LD, only detects oriented chromophores. Upon formation of the reduced dichroism of Eq. (2), $A_{\mathrm{iso}}$ should refer to the same number of molecules as does LD. This often requires correction for the absorption contribution of some fraction of non-associated or randomly distributed chromophores.

*Turbidity dichroism*

Anisotropic turbidity has been considered in a few idealized cases in connection with shear orientation (Meeten 1981; Mayfield and Bendet 1970), however, no general theoretical formalism has yet been derived for partially oriented samples. Numerical calculations of the turbidity dichroism of stiff rods, with the orientation distribution in a Couette shear and within the Rayleigh-Gans approximation (Mikati and Nordén, unpublished) show that turbidity dichroism, in contrast to the absorbance dichroism of Eq. (1), cannot generally be factorized into an orientation factor and a scattering factor. Still there has been experimental evidence that a semi-quantitative description of this kind may be applicable (Hall and Schellman 1982) and the numerical calculations indicate that such a linear relation is justified under certain scattering and orientation conditions. A very similar shape of the turbidity dichroism, $\mathrm{LD}^\tau$, and the turbidity of the isotropic sample, $A_{\mathrm{iso}}^\tau$, as functions of the wavelength should make the reduced linear dichroism, $\mathrm{LD}_r^\tau = \mathrm{LD}^\tau/A_{\mathrm{iso}}^\tau$, for very long rods independent of the wavelength in the non-absorbing wavelength region, in agreement with the experimental findings. Both $\mathrm{LD}_r^A$ and $\mathrm{LD}_r^\tau$ are zero for random solutions and increase monotonically to the respective values corresponding to complete orientation.

Against this background and the consistency within the present investigation, we shall use a linear relation in analogy with Eq. (1) for turbidity linear dichroism:

$$\mathrm{LD}_r^\tau = \frac{\mathrm{LD}^\tau}{A_{\mathrm{iso}}^\tau} = S \times 0.68\,. \quad (3)$$

It must be emphasized that the validity of this equation has so far only been shown to be semi-quantitative. The factor 0.68 corresponds to the polarized limiting scattering of infinite, perfectly parallel rods (compare: Higashi et al. 1963; Mikati and Nordén, unpublished). The influence of the shear gradient will be further discussed below. A special study in which the experimental, ordinary and turbidity dichroisms are correlated to each other is in progress.

*Simulation of shear orientation*

We shall finally compare the time dependence of orientation from the start of shear with that predicted from a single hydrodynamic model for Couette orientation. We shall assume non-interacting and stiff, rod-shaped particles (of infinite axial ratio) and neglecting in the present calculation rotational diffusion. The instantaneous angular velocity of single particle, due to the shear gradient, can then be described (Nordén and Nordh, unpublished) as:

$$\frac{d\Phi}{dt} = \omega_\Phi = 1/2\,(1+\cos 2\Phi)\cdot G \qquad (4)$$

$$\frac{d\Theta}{dt} = \omega_\Theta = 1/2\,(\sin\Theta\cdot\cos\Theta\cdot\sin 2\Phi)\cdot G\,, \qquad (5)$$

where $\Phi$ and $\Theta$ define the orientation of the particle in a Cartesian coordinate system, $X$, $Y$, $Z$; $\Theta$ being the angle between the long-axis of the particle and the Couette rotation axis, $Y$, and $\Phi$ the angle between the direction of the shear gradient, $Z$, and the projection of the long-axis of the particle on the $XZ$ plane, $X$ being the shear direction (Fig. 1). The orientation model can be visualized by first considering the two dimensional case: a rod-shaped particle lying in the $XZ$ plane at an angle $\Phi$ relative to the $Z$ axis. If $\Phi$ differs from 0 the particle will have its ends in stream lines, moving with different velocities: $v \pm 1/2\,GL\cos\Phi$, where $v$ is the velocity of the centre of the rod and $L$ the rod length. Its angular velocity, which is independent of the rod length, is then described by Eq. (4). For the three-dimensional case one obtains, in addition, Eq. (5). Equations (4) and (5) were solved numerically by considering an ensemble of 20,000 randomly generated rods, initially distributed isotopically in the gradient $0 < \Theta < \pi/2$, $-\pi/2 < \Phi < \pi/2$. The dynamics of the orientational distribution was then calculated from Eq. (4) and (5) using sufficiently small time steps to obtain stable solutions. The time development of the orientation factor $S$ is obtained by averaging over the ensemble at different times. For the present geometry, $S$ can be expressed (Wada 1972):

$$S = 3/2\langle\sin^2\Theta\rangle - 1/2\langle\sin^2\Theta\cdot\cos 2\Phi\rangle - 1\,. \qquad (6)$$

## Results

*Intrinsic chromophores*

The LD of the intrinsic chromophores of shear-oriented microtubules was studied in the wavelength region 240–400 nm after correction for the contribution from the background turbidity $LD^\tau$. The absorption dichroism was assumed to add to the background light scattering, according to Eq. (7a). The wavelength dependence of $LD_\tau$ was estimated by linear regression of Eq. (7b), fitting it to the apparent LD curve in the non-absorbing long-wavelength region:

$$LD_{total} = LD^A + LD^\tau \qquad (7a)$$

$$LD^\tau(\lambda) = a\lambda^{-k}\,, \qquad (7b)$$

where the exponent $k$ was generally identical to that of the unpolarized turbidity, however, varying between preparations, $k = 2.8-3.5$. The LD due to absorption was thus obtained when the extrapolated $LD^\tau(\lambda)$ values were substracted from the measured apparent LD. To calculate $LD_r^A$, the reduced linear dichroism spectrum of shear oriented microtubules (see Eqs. (2) and (3)) the total absorption, $A$ of the unpolymerized microtubule protein solution was first measured in the absence of added excess GTP. A characteristic spectrum is shown in Fig. 2. The reduced dichroism due to absorption was positive and fairly high, $LD_r^A$ varying between 0.1–0.4 in the wavelength region 290–300 nm.

Although the amplitude of the linear dichroism signal depends on the shear gradient, the shape of the absorption dichroism spectrum was within measurable errors the same at low and at high gradients.

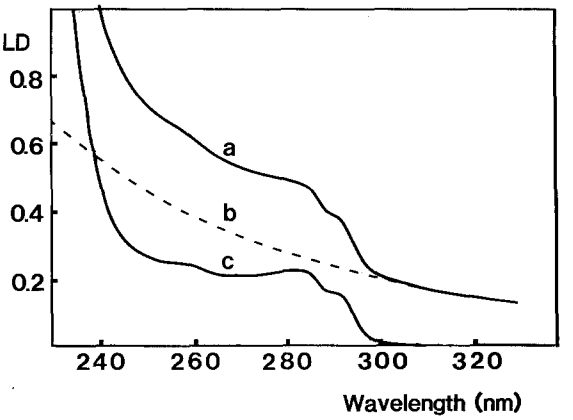


**Fig. 2.** Flow LD of intrinsic chromophores. Microtubules, 0.75 mg/ml assembled in buffer (0.1 *M* Pipes · NaOH, 0.5 m*M* $MgSO_4$ with 1 m*M* GTP at pH 6.8) in Couette cell. Assembly was initiated by raising the temperature from 10° to 35 °C. The shear gradient was $G = 1\ s^{-1}$. The experimental (*a*) and the corrected (*c*) spectra and the calculated turbidity (*b*). (LD normalized to 1 cm path-length)

This indicates that the local structure, i.e. the orientation of the intrinsic chromophores of the microtubules, was not measurably perturbed by the shear. The same spectrum was also obtained from the thermal-gradient oriented samples. One advantage of linear dichroism is the possibility of measuring at different concentrations of added GTP, in spite of a high absorption as only oriented, microtubule-associated GTP contributes to the LD signal.

*Assembly measured by flow dichroism*

At 350 nm microtubule proteins have no absorption and the observed dichroism is entirely due to the anisotropic turbidity. The development of a $LD^{\tau}$ signal at 350 nm at a constant shear gradient was found useful for monitoring the assembly of microtubules (Fig. 3). The same overall features as seen by $LD^{\tau}$ were also seen when assembly was monitored by the change in turbidity, $\Delta A^{\tau}$. However, in contrast to ordinary turbidity, $LD^{\tau}$ was practically zero at the starting point, showing that low-temperature aggregates do not contribute significantly. As will be discussed, the optimal $LD^{\tau}$ at steady state of assembly in Fig. 3 most likely corresponds to more or less perfect orientation of the microtubules. Moreover, the shear orientation did not seem to influence the process of microtubules assembly and the same $LD^{\tau}$ signal was obtained whether the gradient was applied initially or at the steady-state of assembly. Furthermore, the microtubules apparently had the same appearance, as estimated from negatively stained electron microscopy samples taken at different gradients and time intervals.

In contrast to 'ordinary' turbidity measurements, where a residual turbidity generally remains after disassembly of the microtubules the $LD^{\tau}$ signal disappears almost completely upon cooling to 4 °C or adding $Ca^{2+}$ to a final concentration of 5 m*M*. This is expected since only orientable, light scattering polymers can contribute to $LD^{\tau}$. This was also confirmed by the observation that the very turbid solution of denatured microtubule proteins, kept at 45 °C, did not contribute with any significant linear dichroism.

Figure 4 shows the variation of $LD^{\tau}$ as a function of the protein concentration of microtubules at steady state of assembly. A virtually linear relationship was obtained for $LD^{\tau}$, as for the turbidity (not shown), but with a slightly higher apparent critical protein concentration: 0.17 mg/ml, instead of 0.12 mg/ml as found from the turbidity. The high sensitivity of linear dichroism is apparent as even at low protein concentrations a reliable signal to noise was obtained.

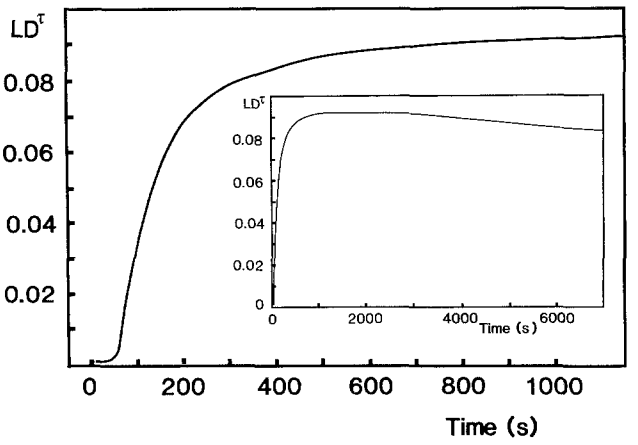


**Fig. 3.** Microtubule assembly. Assembly of microtubule proteins (0.57 mg/ml in buffer without GTP in a Couette cell kept at 35 °C) initiated by addition of GTP to a final concentration of 1 m*M*. During assembly, monitored by $LD^{\tau}$ at 350 nm, a constant shear gradient of $G = 100\ s^{-1}$ was applied. (LD normalized to 1 cm path-length)

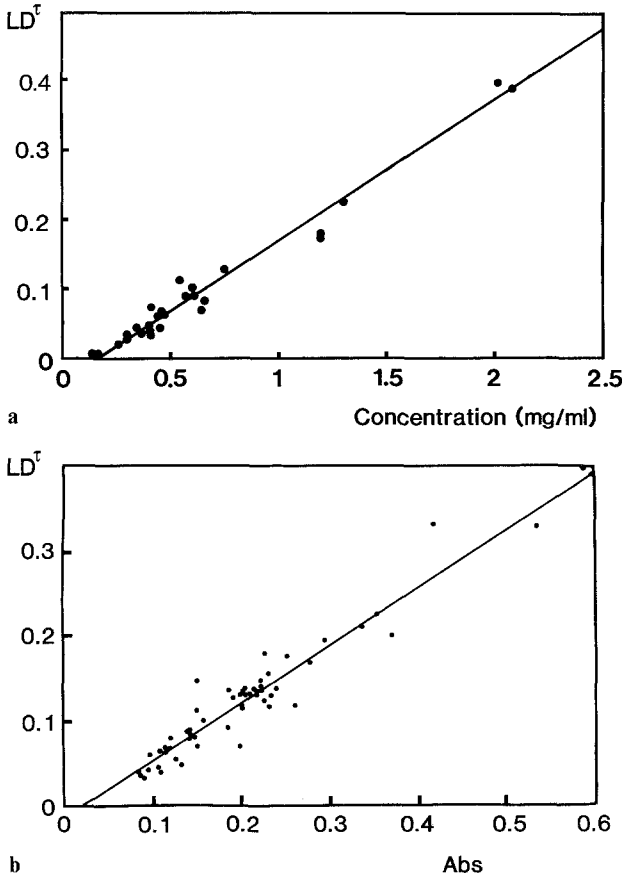


**Fig. 4a and b.** Concentration dependency of assembly. Microtubules at steady state of assembly under the same conditions as in Fig. 2 at $G = 100\ s^{-1}$. **a** $LD^{\tau}$ at 350 nm versus the protein concentration. The critical concentration, 0.16 mg/ml (linear regression: $n = 27$, $R = 0.98$, slope = 0.20 ml/mg). **b** $LD^{\tau}$ versus $\Delta A^{\tau}$. Different concentrations from five different MTP preparations were used. The slope (0.68) was obtained by linear regression ($n = 60$, $R = 0.97$). (LD normalized to 1 cm path-length)

In Fig. 4b, $LD^{\tau}$ is plotted versus $AA^{\tau}$ for a number of different preparations. At a shear gradient giving saturated orientation an essentially linear relationship corresponding to: $LD_r^{\tau} = LD^{\tau}/A^{\tau} = 0.68$ (i.e. $S = 1$ in Eq. (3)), is obtained. $LD_r^{\tau}$ is thus practically independent of the protein concentration for $G = 10-100\ s^{-1}$.

*LD as a function of the shear gradient*

In Fig. 5 the $LD^{\tau}$ of shear-oriented microtubules at the steady-state of assembly is plotted against the shear gradient in the interval $G = 10^{-3}-10^{3}\ s^{-1}$. In this interval the process of orientation was found to be completely reversible. Saturation was obtained at $G = 10-100\ s^{-1}$. However, gradients higher than $1{,}000\ s^{-1}$ introduced irreversible damage of the microtubule structure, as evidenced from a decrease in $LD^{\tau}$ and thus a decreased orientability.

In the lower gradient region, where $LD^{\tau}$ was not optimal and the degree of orientation ($S < 1$ in Eq. (3)) was incomplete, a significant dependency on the protein concentration was observed. As seen from the insert in Fig. 5, at a constant and low gradient, $G = 0.03\ s^{-1}$, $LD^{\tau}$ (and thus the degree of orientation) clearly increases with the protein concentration.

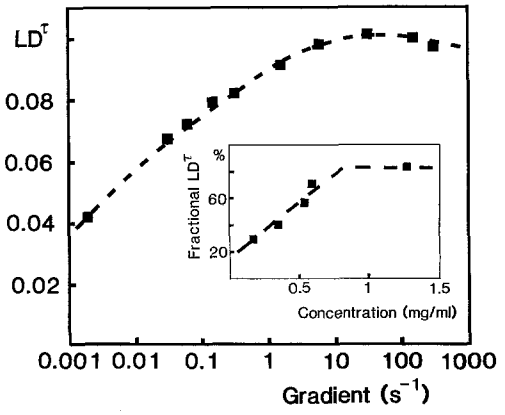


**Fig. 5.** LD as a function of gradient and concentration. $LD^{\tau}$ at 350 nm of microtubules, 0.60 mg/ml, at steady state of assembly (the same assembly conditions as in Fig. 2) versus the shear gradient. *Insert:* fractional $LD^{\tau}$ at 350 nm (= the ratio in % between $LD^{\tau}$ at a fixed low gradient ($G = 0.03\ s^{-1}$) and the optimal $LD^{\tau}$ at $G = 30\ s^{-1}$) versus the microtubule protein concentration. (LD normalized to 1 cm path-length)

*Time-development of orientation with shear*

The $LD^{\tau}$ signal due to orientation of microtubules develops very rapidly upon applying the shear force. With a high shear gradient the steady-state orientation was reached almost within the time response of the instrument (0.1 s, see Instrumentation). However, at low gradients, because of the slow reorientational dynamics it was possible to follow the development of the orientation as a function of time. Figure 6 shows the rise of $LD^{\tau}$ with time when a shear gradient of $0.03\ s^{-1}$ was applied to a solution at rest, and also the subsequent relaxation to random orientation after stopped-shear. The figure also presents the calculated orientation according to the model (Eqs. (4) and (5)).

*Stopped shear orientation relaxation*

Upon immediate stop of the orienting shear field a relaxation to random orientation of the microtubules takes place. The relaxation curves (an example is given in Fig. 7) are not single exponentials, as found

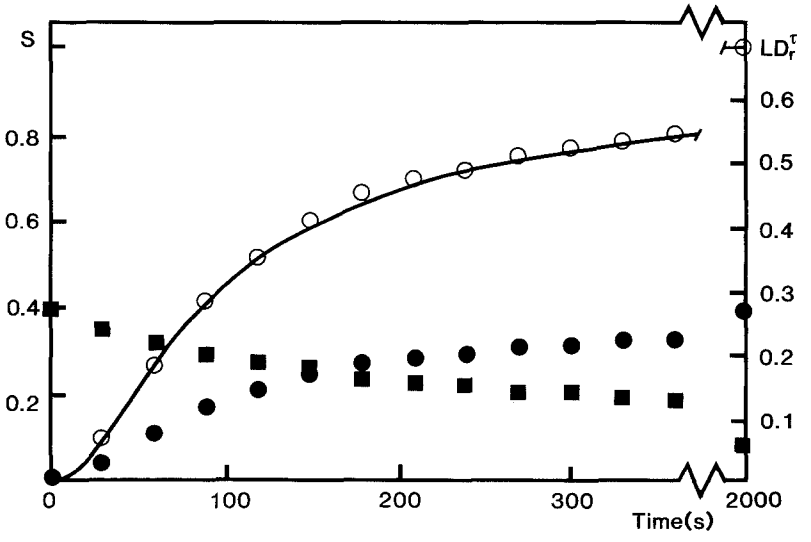


**Fig. 6.** Flow orientation dynamics. Microtubules, 0.75 mg/ml, assembled in the Couette cell with a thermostated outer-cylinder under the same conditions as in Fig. 2 at $G = 0$. At steady state of assembly the microtubule were orientated by a low gradient, $G = 0.03\ s^{-1}$ recorded by $LD^{\tau}$ at 350 nm (●). After stop of shear (■), the microtubules return to random orientation. The solid curve presents the model computed for orientation of stiff rods, Eq. (4–6) and the open circles measured values normalized to $S = 1$

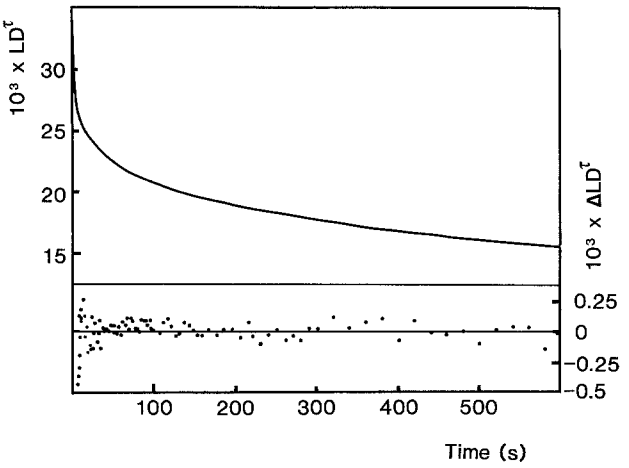


**Fig. 7.** Relaxation of shear-oriented microtubules: Assembled microtubules, 0.37 mg/ml, in the Couette cell with a thermostated outer-cylinder under the same conditions as in Fig. 2. After shear orientation by $G = 100\ s^{-1}$ the rotation was stopped and the decline in $LD^{\tau}$ at 350 nm recorded versus time. The curve was fitted to a tri-exponential with a residual term = offset: 13.7 with $P_i = 8.55$, 4.64, 7.11 respectively and $T_i = 393.7$, 39.1 and 3.0 s, respectively. *Below:* the regression error. (LD normalized to 1 cm path-length)

**Table 1.** Stopped-shear orientation relaxation of microtubules by linear dichroism

| Relaxation time | | | Relative contributions $P_i/LD^{\tau} \times 100\%$ | | |
|---|---|---|---|---|---|
| | $T_i$ [s] | Median (93% conf. interv.) | Protein [mg/ml] | | |
| | | | 0.15 | 0.7 | 2.0 |
| Rapid | 3.7 | (2.6–5.5) | 16 | 14 | 9 |
| Intermediate | 39 | (34–45) | 20 | 16 | 8 |
| Slow | 440 | (280–760) | 30 | 21 | 17 |
| Offset | > 4,000 | – | 34 | 50 | 66 |

Data from 11 samples. The experimental conditions were the same as in Fig. 2 after shear at $G = 100\ s^{-1}$

for short DNA, but can be fitted to a multi-exponential decay: $LD^{\tau}(t) = \sum P_i \cdot \exp(-t/T_i)$, where $LD^{\tau}(t)$ denotes the LD signal at time $t$. The pre-exponential factor $P_i$ is the amplitude and $T_i$ a relaxation time constant. Time constants of the orders of 4, 40, 400 and above 4,000 s were obtained for 'rapid', 'intermediate', 'slow' processes and an 'offset', respectively (Table 1). The amplitudes of the pre-exponential factors, reflecting the contributions from the different relaxing processes, showed a virtually linear increase with the protein concentration. Furthermore, the relative contribution from the slowest processes, the offset increases with increasing protein concentration. Above 1 mg/ml the relative contribution from the offset appears to become constant, approximately 60%, indicating the existence of a stable fraction, maintaining a semi-permanent orientation. However, solutions of microtubules which had been shear-oriented for a longer period of time, more than 1 h, showed a less pronounced residual orientation. It should be noted that this was the only measurable shear-induced irreversible change on the microtubule solution in the gradient interval used.

*Thermal gradient*

The convection shear due to the application of a relatively small thermal gradient was found sufficient to effectively orient microtubules. It was found that the flow $LD^{\tau}$ of microtubules in the rotating outer-cylinder Couette cell, after stopped rotation, changes from a positive to a negative LD signal of almost equal magnitude within 5–10 min. This is an effect of a temperature difference of approximately 5 °C over the gap between the outer- and inner-cylinder walls changing the orientation direction from horizontal to vertical. At low protein concentration, 0.2 mg/ml, the negative LD signal frequently showed fairly rapid oscillations, possibly due to the formation of local convection cells. With higher protein concentrations, 0.7 mg/ml, a slower reorientation towards almost saturated vertical orientation was observed. The thermal vertical orientation was effectively cancelled by a very small horizontal shear: e.g. with $G = 0.01\ s^{-1}$ (0.0033 rpm) and 0.85 mg/ml, as much as 17% of the maximal positive $LD^{\tau}$ was obtained. Thermal-gradient induced orientation is an important observation, showing a possible method for producing oriented microtubules, but also how easily temperature differences can perturb the structure of microtubule solutions.

## Discussion

*Intrinsic chromophores*

The high $LD_r^A$ value of the intrinsic chromophores in oriented microtubules suggests relatively uniform orientation. A similar result was found by Taniguchi and Kuriyama (1978), however in 30% glycerol and at a higher shear rate. Tubulin contains a large number of aromatic amino acid residues absorbing in the ultraviolet wavelength region. The main contribution to the absorption at 280 nm derives from 36 tyrosine and 8 tryptophan residues in each tubulin hetero-dimer. This complexity may prevent any detailed conclusions about the arrangements of the chromophores.

A weak dichroism band from guanine in GTP (2 GTP per tubulin dimer) should in principle contain useful information about the orientation of tubulin in the microtubule structure. Although GTP was present in a more than 50-fold excess over tubulin, $LD^A$ only shows the contribution of oriented, bound guanine. The transition moments of guanine in the UV region are well established: a transition at 248 nm is essentially long-axis and in-plane polarized, while a second band at 279 nm has more or less short-axis polarization (Matsuoka and Nordén 1982). The positive $LD^A$ contribution at 250 nm should then suggest a more parallel orientation of the long-axis of guanine relative to the microtubule axis.

*Turbidity dichroism*

The results show that flow dichroism ($LD^\tau$) due to anisotropic turbidity is useful for quantitative measurements of assembled microtubules (Fig. 3). $LD^\tau$ has advantages over ordinary turbidity measurements which are affected by the presence of scattering but virtually non-orientable species such as aggregates of denatured tubulin. This was found particularly in dilute or aged microtubule solutions.

Microtubules are apparently relatively strong structures since electron microscopy indicates that they remain unaffected by the shear forces required for orientation. The shear degradation effects involved in passing microtubule solutions through a syringe needle require significantly higher gradients than applied in this study. Scanning up-and-down the shear gradient did not give any measurable hysteresis effects in $LD^\tau$ for gradients below $1{,}000\,s^{-1}$: i.e. the same $LD^\tau$ vs. gradient was obtained whether the gradient was increased or decreased.

In the Couette cell with the rotating inner cylinder a certain decrease in $LD^\tau$ was found at gradients higher than $100\,s^{-1}$ (Fig. 5). In the cell with the rotating outer cylinder the decrease was much less pronounced. The decrease is not due to shear-degradation of microtubules, but can be explained by so-called Taylor centrifugal instability (Kasai and Oosawa 1972).

It is finally interesting to note that the gradient interval $10-100\,s^{-1}$ where the perturbation from shear gives complete orientation corresponds to the range of the falling ball 'low-shear' viscometry (Pollard 1982).

The orientation of microtubules in solution was practically complete in the optimal shear range, $G = 10-100\,s^{-1}$ as judged from the saturation behaviour (Fig. 5) and the limiting reduced dichroism $LD'_r = 0.68$. This value is also in agreement with the theoretical value of perfectly oriented rods. This very high degree of orientation under shear in solution cannot be expected to remain in samples taken for electron microscopy as manipulation and thermal effects easily induce uncontrolled re-orientation.

It is relevant to compare the orientational behaviour of microtubules with other shear-orientable biopolymers. Besides microtubules, as shown in this report, only *F*-actin (Kasai and Oosawa 1972) has been found to be effectively oriented by shear. In contrast, rather flexible polymers such as DNA (Nordén and Tjerneld 1976), myosin and tropomyosin (Kasai and Oosawa 1972) show rather inefficient orientation even at extremely high shear fields. Also a stiff rod-shaped biopolymer such as tobacco mosaic virus seems to be only partially oriented by shear (Mayfield and Bendett 1970). Comparison with *F*-actin in fact indicates that the extraordinary orientability of microtubules is unique among biopolymers. This property may be related to a greater stiffness and length of the microtubules, possibly assisted by ordering effects of inter-microtubule interactions.

*Microtubule interactions*

The limiting value of 0.68 was obtained at optimal shear gradients, ($G = 30-100\,s^{-1}$) irrespective of the protein concentration (cf Fig. 4), suggesting that the microtubules become effectively oriented in dilute as well as in concentrated solutions. In contrast, we find that at very low gradients, where the orientation is incomplete, the degree of orientation was dependent on the microtubule concentration and rapidly increases with the protein concentration (Fig. 5). This behaviour may be explained by an increasing frequency of mutual entanglements of the long, rather stiff microtubules, hindering free rotation. A similar conclusion has been made by Gethner and Gaskin (1978), from studies of translational diffusion of random solutions of microtubules by dynamic light scattering. They suggest that such a solution may be described as a very loose network of entangled strands. Also, microtubule associated proteins may contribute to the orientational behaviour; it has been proposed that they may act as bridging structures with other cytoskeletal components (Dustin 1984).

*Orientation mechanism*

Orientation relaxation, generally with electric fields, has been widely used for the study of various macromolecules for several decades, but, as far as we

know, never on microtubules. We find that the relaxation upon stop of shear contains at least three components (Fig. 7, Table 1), indicating a very complex reorientation process. The relaxation behaviour can be interpreted in terms of *different fractions*, such as free microtubules and clusters, or, which is more plausible, different *physical reorientation processes* in the solution. Two possible such processes are: (a) A fast individual (*local*) reorientation of each microtubule with its rotational freedom defined by a surrounding free volume, (b) a slower, coupled (*long-range*) reorientation of the microtubules due to their mutual interaction.

The fast components ($T = 4$ and 40 s) seem to be more important at lower protein concentrations. For the slow components, as shown in Table 1, higher protein concentrations appear to stabilize a semi-permanent orientation. Both for the fast and the slow components the concentration behaviour is consistent with considerable entanglement between microtubules. There is an indication of a saturation at concentrations higher than approximately 1 mg/ml. An indication of a saturation behaviour is also found in Fig. 5, at a similar concentration level. These observations may be related to the remarkably high values noticed in the low-shear falling ball experiments (Pollard 1982).

We find it relevant to discuss the obtained rotational relaxation times in terms of 'characteristic lengths', $L$ according to the Perrin-Broersma equation for a stiff rod (Broersma 1960):

$$\Theta = \frac{3kT}{\pi \eta_0 L^3} \cdot (\ln L/b - 1.57 + 7(1/(\ln(L/b)) - 0.28)^2), \quad (8)$$

where $T$ is the absolute temperature, $\eta_0$ is the solvent viscosity and $\Theta$ is the rotational diffusion constant, which is calculated from $\Theta = 1/(6\tau_i)$ with $\tau_i$ the relaxation time. The choice of the rod thickness, $b$, was not critical: it was taken to 25 nm. The observed relaxation times, $\tau_i = 440$, 40 and 4 s correspond to the lengths: 40, 15 and 7 μm, respectively. Possibly, only the one corresponding to the rapid relaxation process, may have a physical meaning. It corresponds to the reorientation of an individual microtubule in a state of high orientation. It is comparable with the lengths of microtubules frequently observed in electron micrographs (Kristofferson and Purich 1981). The other, slower relaxation processes may be related to the increasing degree of entanglements when the microtubules become less oriented.

Let us finally compare the experimental orientation rise function with that calculated from our model (Eqs. (4), (5) and (6)). As seen from Fig. 6 the experimental and theoretical orientation functions have very similar shapes and if scaled to the same final, steady state orientation the curves nicely overlap each other. Regarding that we have neglected the influence of rotational diffusion, the agreement is remarkable. The need for scaling could suggest the presence of a fraction which is difficult to orient at the applied low shear gradient, but could also be an effect of the randomizing diffusion.

In *conclusion* this study demonstrates the potential of the LD technique for measuring stationary as well as dynamic orientation of microtubules and shows:

1. An extremely small macroscopic shear force field (or thermal convection) is sufficient to produce effective orientation of microtubules.
2. LD has an advantage over other methods for studying microtubules in that it is insensitive to unorientable aggregates.
3. A complex, multi-exponential reorientation behaviour indicates considerable interactions between the microtubules.
4. The main features of the flow orientation dynamics can be simulated by a simple model for rigid rods.
5. Efficient orientation is already observed at low gradients ($G = 1\ s^{-1}$). Only at high gradients ($G > 1{,}000\ s^{-1}$) is irreversible degradation observed.

*Acknowledgements.* This work has been supported by grants from the Swedish Natural Science Research Council (JD, BN) and Bengt Lundquist Minne (JN). Thanks are due to Dr. Margareta Wallin for help with the electron microscopy.

## References

Borisy GG, Olmsted JB, Marcum JM, Allen C (1974) Microtubule assembly in vitro. Fed Proc Am Soc Exp Biol 33:167–174

Bradford C (1976) A rapid and sensitive method for the quantitation of microgram quantities of protein utilizing the principle of protein-dye binding. Anal Biochem 72:248–254

Broersma S (1960) Rotational diffusion constant of cylindrical particles. J Chem Phys 32:1626–1631

Davidson A, Nordén B (1976) Aspects on the conversion of Legrand-Grosjean circular dichroism spectrometers to linear dichroism. Chem Scr 9:49–53

Deinum J, Wallin M, Lagercrantz C (1981) Spatial separation of the two essential thiol groups and the binding-site of the exchangeable GTP in brain tubulin. A spin label study. Biochim Biophys Acta 671:1–8

Deinum J, Wallin M, Jensen WA (1985) Biochim Biophys Acta 838:197–205

Dustin P (1984) Microtubules. Springer, Berlin Heidelberg New York

Fredericq E, Houssier C (1973) Electric dichroism and electric birefringence. Oxford University Press, London

Gaskin F, Cantor CR, Shelanski ML (1974) Turbidimetric studies of the in vitro assembly and disassembly of porcine neurotubules. J Mol Biol 89:737–758

Gethner JS, Gaskin F (1978) Dynamic light scattering from solutions of microtubules. Biophys J 24:505–515

Haga T, Abe J, Kurokawa M (1974) Polymerization and depolymerization of microtubules in vitro as studied by flow birefringence. FEBS Lett 39:291–295

Hall SB, Schellman JA (1982) Flow dichroism of Capsid DNA phages. I. Fast and slow T4B. Biopolymers 21:1991–2010

Higashi S, Kasai M, Oosawa F (1963) Ultraviolet dichroism of *F*-actin oriented by flow. J Mol Biol 7:421–430

Hofrichter J, Eaton WA (1976) Linear dichroism of biological chromophores. Annu Rev Biophys Bioeng 5:511–531

Kasai M, Oosawa F (1972) Flow birefringence. Methods Enzymol 26:289–323

Kristofferson D, Purich DL (1981) Time scale of microtubule length redistribution. Arch Biochem Biophys 211:222–226

Matsuoka Y, Nordén B (1982) Linear dichroism studies of nucleic acid bases in stretched poly(vinyl alcohol) film. Molecular orientation and electronic transition moment directions. J Phys Chem 86:1378–1386

Mayfield JE, Bendet IJ (1970) Quantitative flow dichroism. I. Correction for disorientation in a solution of rods. Biopolymers 9:655–668

Meeten GH (1981) Conservative dichroism in the Rayleigh-Gans-Debye approximation. J Colloid Interf Sci 84:235–239

Nordén B (1978) Applications of linear dichroism spectroscopy. Appl Spectrosc Rev 14(2):157–248

Nordén B, Seth S (1985) Critical aspects of measurement of circular and linear dichroism. A device for absolute calibration. Appl Spectrosc Rev 39:647–655

Nordén B, Tjerneld F (1976) High sensitivity linear dichroism as a tool for equilibrium analysis in biochemistry, stability constant of DNA ethididium bromide complex. Biophys Chem 4:191–198

Nordén B, Tjerneld F (1982) Structure of methylen blue-DNA complexes studied by linear and circular dichroism spectroscopy. Biopolymers 21:1713–1734

Pollard TD (1982) A falling ball apparatus to measure filament cross linking. Methods Cell Biol 24:301–311

Tanichuchi M, Kuriyama R (1978) Ultraviolet flow dichroism of brain microtubules. Biochim Biophys Acta 533:538–541

Thulstrup EW (1980) Aspects of the linear and magnetic circular dichroism of planar organic molecules. In: Berthier G, Dewar MJS, Fischer H, Fukuii K, Hartmann H, Jaffe HH, Jortner J, Kutzelnigg W, Ruedenberg K, Scrocco E, Zeil W (eds) Lecture Notes in Chemistry, Vol 14. Springer, Berlin Heidelberg New York

Wada A (1972) Dichroic spectra of biopolymers oriented by flow. Appl Spectrosc Rev 6:1–29

Wada A, Kozawa S (1964) Instrument for the studies of differential flow dichroism of polymer solutions. J Polymer Sci A 2:853–864

Wilson R, Schellman J (1978) The flow linear dichroism of DNA: comparison with the bead spring theory. Biopolymers 17:1235–1248